J. Plant Biol. (2018) 61:227-240
DOI 10.1007/s12374-017-0410-7

ORIGINAL ARTICLE

Functional Analyses of *PtROS1*-RNAi in Poplars and Evaluation of Its Effect on DNA Methylation

Ali Movahedi[1,†], Ming Sang[1,†], Jiaxin Zhang[3], Kourosh Mohammadi[1], Weibo Sun[1], Amir Almasi Zadeh Yaghuti[1], Saeid Kadkhodaei[2], Honghua Ruan[1] and Qiang Zhuge[1,*]

[1]*Co-Innovation Center for Sustainable Forestry in Southern China, Key Laboratory of Forest Genetics and Biotechnology, Ministry of Education, Nanjing Forestry University, Nanjing 210037, China*
[2]*Institute of Tropical Agriculture, Putra Malaysia University, 43400 UPM Serdang, Selangor, Malaysia*
[3]*Department of Food Science and Technology, Ginling College, Nanjing Normal University, Nanjing 210097, China*

Received: October 30, 2017 / Accepted: April 16, 2018

Abstract DNA methylation occurs mostly at the C5 position of dinucleotide symmetric CpG sites in genomic DNA. A balance is maintained in the plant genome between DNA methylation mediated by RNA-directed DNA methylation (RdDM) and DNA demethylation mediated by the DEMETER (DME) protein family and REPRESSOR OF SILENCING (ROS1). We used double-stranded RNA (dsRNA) silencing to suppress ROS1 protein expression in 'Nanlin895' (*Populus deltoides* × *Populus euramericana* 'Nanlin895'). Leaves of WT and transformant poplars revealed more symmetric methylation on CpG sites than roots and stems. In addition, leaves of transformant poplars revealed more methylated CpG sites in both *5.8S* rDNA and histone *H3* compared to WT types via 0, 50 and 100 mM NaCl treatments. In asymmetric methylation sites, transformant poplars exhibited more methylated CpHpG and CpHpH contexts than WT poplars. On the other hand, hypermethylation induced by *PtROS1*-RNAi construct resulted in pleiotropic phenotypic changes in transgenic poplars. The percentage of wavy leaves was increased maximum by ~45% in transgenic poplars. Also, the number of leaves was increased by ~200 number in transformants. Furthermore, shooting (%) and rooting (%) was decreased in transgenic poplars versus WT.

Keywords: Bisulfite sequencing, DNA methylation, Gene silencing, *PtROS1*

Introduction

Epigenetic genome modification and chromatin remodeling play a major role in the regulation of plant development (Feng et al. 2010). Heterochromatin and euchromatin are formed by chromatin remodeling, which involves processes such as histone modification and cytosine methylation. Roudier et al. (2011) described that four main chromatin regions involved repressed genes, intergenic regions, silent repeat elements, and active genes are be subjected to cytosine methylation and histone modification. The effect of cytosine methylation on gene expression is dependent on the location of methylation. DNA methylation in the body of genes is associated with gene expression and varies among species (Lauria and Rossi 2011; Vining et al. 2012), while cytosine methylation in promoter regions is associated with decreased gene expression (Zhang et al. 2006). Lippman et al. (2004) reported that a high level of cytosine methylation silences transposable elements located in heterochromatin. Moreover, reduced cytosine methylation led to reactivation of transposable elements.

DEMETER (DME), DME-LIKE proteins (DML2 and DML3), and REPRESSOR OF SILENCING (ROS1) are involved in demethylation activities in the plant genome (Choi et al. 2002; Furner and Matzke 2011). ROS1 was identified by Gong et al. (2002) via mutant screening of repetitive transgenes, including luciferase, driven by the *RD29A* promoter. In plants, DML2, DML3, and ROS1 demethylate DNA to protect hypermethylation loci (Penterman et al. 2007). A balance is maintained between ROS1, which mediates demethylation, and the RNA-directed DNA methylation (RdDM) pathway (Gao et al. 2010). Furthermore, it has been shown in wild-type (WT) plants, ROS1 counteracts small interfering RNAs involved in DNA methylation, leading to DNA demethylation (Gong et al. 2002). The RdDM pathway is

[†]These authors contributed equally in this work.

*Corresponding author; Qiang Zhuge
Tel : +86-25-85428701
E-mail : qzhuge@njfu.edu.cn

a mechanism of epigenetic modification in eukaryotes which contains several important genes involved in regulating DNA methylation (Kapoor et al. 2005; Movahedi et al. 2015a). In addition, ROS1 demethylates silenced transgenes and endogenous loci during plant development responding to environmental stress (Penterman et al. 2007; Gehring et al. 2009). The mutant *ros1* is associated with hypermethylation at various regions throughout the genome, resulting primarily in silencing of proximal genes (Lister et al. 2008). Gao et al. (2010) reported that in the presence of the *ros1* mutation, heavy methylation occurs in all sequences, including CpG, CpHpG, and CpHpH, where H represents any nucleotide without guanine. Dinh et al. (2014) reported that histone *H3* is one rich lysine 9 dimethylation and repetitive DNA through plant genomic DNA, which is related to transcriptional silencing mechanisms and curtail target to maintain genome stability via DNA methylation in plants. Studies on *ros1* mutant showed that ROS1 demethylates DNA via DNA glycosylase activity through a base excision repair mechanism (Agius et al. 2006), leading to controls DNA methylation in many eukaryotes (Tariq and Paszkowski 2004). In plants, ROS1 regulates several transposons and genes via demethylase activities responding to environmental signals to improve survival (Zhu et al. 2007). Questa et al. (2013) reported that in plant development and during the either germination or post-germination steps, ROS1 binds to polIV, resulting in chromatin remodeling in *5.8S* rDNA.

Environmental stresses change the level of expression of regulator genes, biochemical properties and chromatin remodeling to affect on both plant growth and productivity (Nakashima et al. 2009; Movahedi et al. 2015b; Movahedi et al. 2015c). In addition, Feng et al. (2010) confirmed that chromatin remodeling, as a heritable epigenetic modification, regulates the expression of plant genome responding to environmental stresses. Epigenetic modifications include heterochromatin and euchromatin remodeling and also DNA repair mediated by histone modification and cytosine methylation in intergenic regions, repressed genes, active genes, and repeat elements (Roudier et al. 2011).

Poplar was the first woody diploid tree, which has been transformed. It has been shown that poplar is one high efficient and stable in expression of transgenes. Therefore, it was called as a model for transgenic plants. This is the first study on silencing of expression of ROS1 with the aim of assessing the role of ROS1 in DNA methylation of histone *H3* and *5.8S* rDNA genes in poplar plants using a *PtROS1*-RNAi construct.

Results

Identification of the Gene Encoding PtROS1 in *P. trichocarpa*

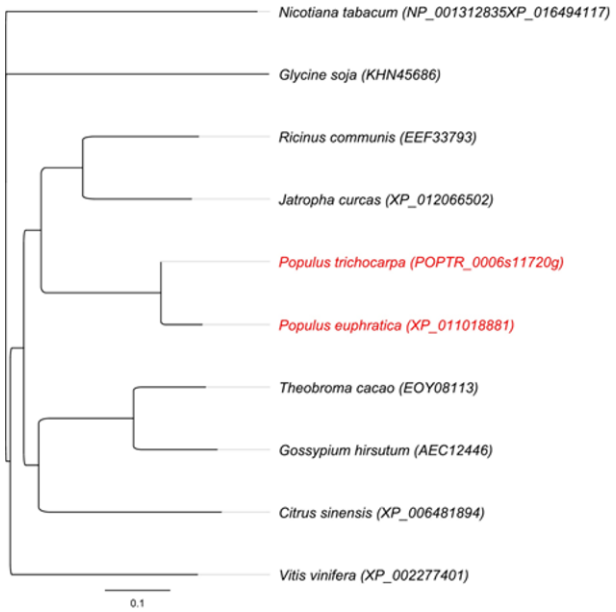

Fig. 1. Identification of the *P. trichocarpa ROS1* (*PtROS1*) gene. Phylogenetic tree analysis was carried out based on the results of homology searches using the amino acid sequence alignment function in CLC Genomics Workbench 3 software. Bootstrap analysis was performed using 1,000 replicates to evaluate the reliability of the various phylogenetic groups.

We carried out a BLAST homology search using the ROS1 protein sequence from *Populus euphratica* (Accession No. XP_011018881) and the corresponding sequences of 10 plant species: *Vitis vinifera* (XP_002277401), *Nicotiana tabacum* (NP_001312835 XP_016494117), *Citrus sinensis* (XP_006481894), *Lonicera japonica* (ALA55997), *Jatropha curcas* (XP_012066502), *Gossypium hirsutum* (AEC12446), *Theobroma cacao* (EOY08113), *Ricinus communis* (EEF33793) and *Glycine soja* (KHN45686) containing domains with similarity to the conserved PtROS1 domain from *P. trichocarpa* (POPTR_0006s11720g) to identify PtROS1 homologs (Fig. 1). The PtROS1 consensus sequence was identified by alignment of the highly conserved domain of ROS1 with that of the *P. euphratica* homolog (Fig. S1). We performed dot plot and isoelectric charge point analyses of PtROS1 and the ROS1 homolog of *P. euphratica* to verify the similarity between them (Fig. S2).

Silencing of *PtROS1* Homolog Expression in Nanlin895 Poplar

The *PtROS1*-RNAi construct was used to transform Nanlin895 poplar via the Agrobacterium method (Fig. S3 and 4). Analysis of off-targets have been performed throughout whole genome of *P. trichocarpa* (Fig. S5). Off-targets have been selected after deleting repeat sequences, sequences located on introns and sequences with coverage less than

15%. In addition, primers have been designed to perform RT-qPCR for comparing the effect of *PtROS1*-RNAi on the expression of on-targets and off-targets (Fig. S5).

Results revealed that our RNAi construct have no impact on genes related to the detected off-targets, when they have been shown expressed normally. The plasmid pGWB9 (empty vector) and ligated pGWB9:*PtROS1*-RNAi were digested by *Hind*III enzyme to verify proper ligated plasmids (Fig. S6A). Furthermore, transformed pGWB9: *PtROS1*-RNAi plasmid was digested by *Hind*III and *Asi*SI enzymes to verify ligation leading to observe two bands 12547 and 845 bp (*PtROS1*-RNAi caset) (Fig. S6B). Genomic DNA was extracted from putative transformed plants to perform colony PCR and reveal amplified fragments 3764 bp (Fig. S6C). The 3764 bp fragments were then purified from gels and digested again by *Hind*III and *Asi*SI enzymes to confirm constructed RNAi caset (Fig. S6D).

RT-PCR has been carried out to compare the expression of *PtROS1* gene in WT and transformed plants introduced by 50 mM NaCl, regarding to *β-actin* as a control (Fig. 2A, B). WT revealed more expression of *PtROS1* in comparing with *PtROS1*-RNAi transformants. In addition, SDS-PAGE and western blotting assays were carried out to confirm silencing PtROS1 homolog expression in transformants compared to WT poplars (Fig. 3). Therefore, we resulted that the RNAi mechanism via dsRNA strategy was able to repress transcript

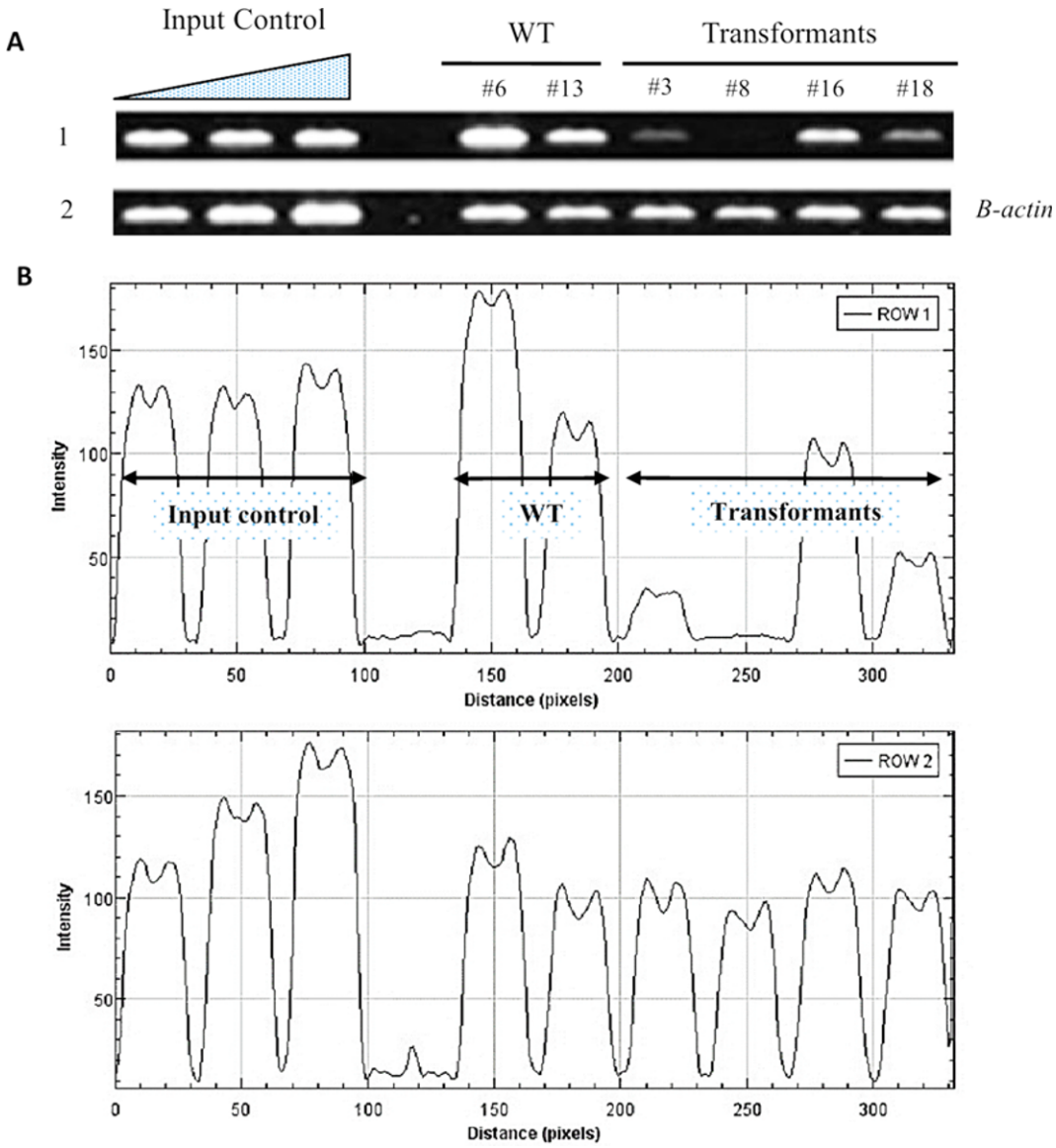

Fig. 2. *PtROS1* expression in transgenic plants assayed by RT-PCR. (A) *PtROS1* expression in transformants was ~25% that of controls. Control cDNA in increasing concentration (two fold increments) was used to normalize band intensities. To normalize band intensities to the cDNA concentration present in the reactions, actin primers were used in control reactions. Numbers above lanes refer to individual plants. (B) Intensity of *PtROS1* expression in WT and transformants.

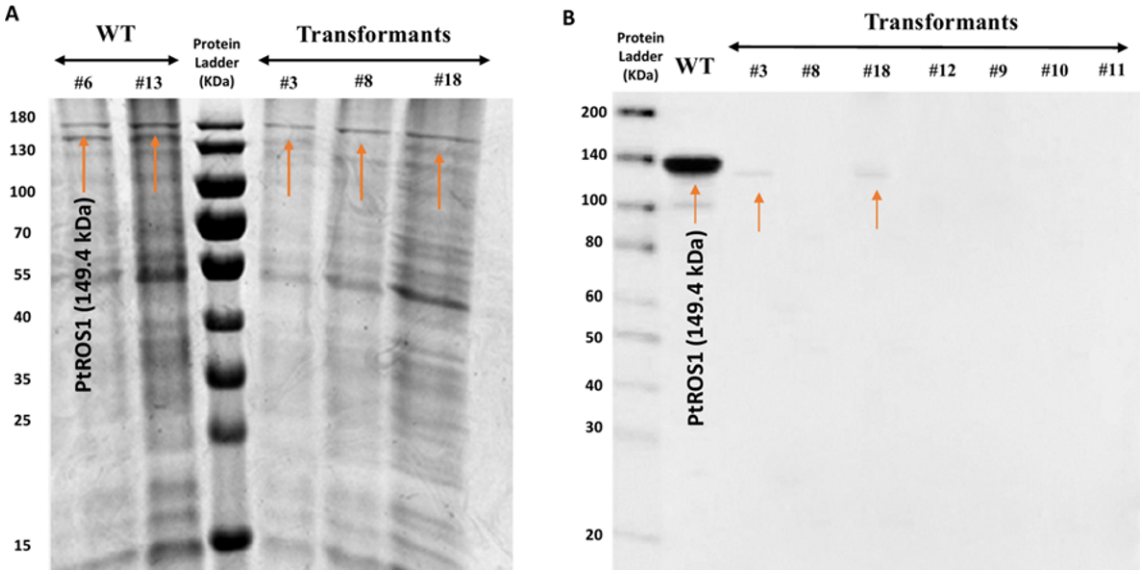

Fig. 3. (A) SDS-PAGE analyses to detect ROS1 protein in WT and transformants. (B) Western blotting analyses to detect ROS1 protein in WT and transformant poplars. Numbers above lanes refer to the individual plants.

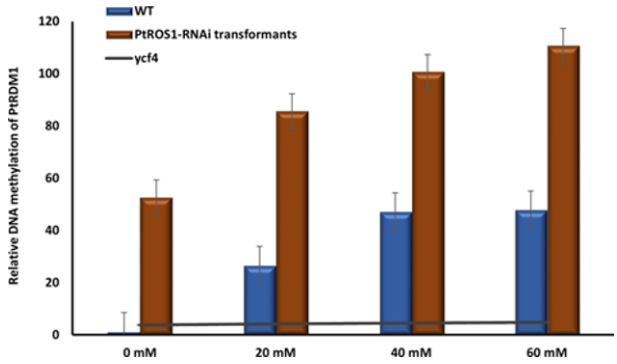

Fig. 4. Demethylase activities of PtROS1 using RE-qPCR. Genomic DNA was digested by *Hpa*II (sensitive methylation) to prime *PtRDM1* gene. *Ycf4* gene was used as control.

PtROS1 in Nanlin895 poplar to forward other examination.

qPCR and Functional Analysis of *PtROS1* Expression

RE-qPCR was carried out to reveal demethylates activities of PtROS1 (Fig. 4). In this assay, we digested genomic DNA from WT and transformants by *Hpa*II followed by priming *PtRDM1* in 0, 20, 40 and 60 mM NaCl treatments. In WT poplars, increasing of DNA methylation via NaCl treatments caused to inhibit of *Hpa*II digestion, leading to increase expression of *PtRDM1* gene. *PtROS1*-RNAi transformants, including the lowest demethylase activities, revealed hypermethylated *PtRDM1* gene resulting in increased expression of *PtRDM1* much more than WT poplars.

Furthermore, qPCR was performed to quantify endogenous *PtROS1* gene expression in both WT and transgenic poplars under 0, 50 and 100 mM NaCl treatments. In natural conditions (0 mM NaCl treatment), WT poplars revealed the expression of *PtROS1* by ~85%, ~60% and ~%50 in leaves, roots and stems. These expressions were increased by ~45%, ~70% and ~85% in leaves, roots and stems by increasing the NaCl treatments (50 and 100 mM). As opposed to WT poplars and in normal conditions, the *PtROS1*-RNAi caused to decrease the expression of *PtROS1* in transgenic lines averagely, by ~65%, ~45% and ~37% in leaves, roots and stems. These expressions were decreased averagely by ~30%, ~18% and ~8% in leaves, roots and stems by increasing the NaCl treatments (Fig. 5).

The largest proportion of the ROS1 orthologs was involved in biological processes including DNA repair and modification by methylation and excision repair. In addition, ROS1 was found to play an important role in the cellular response to stress and stimulators (Fig. S7).

Downregulation of ROS1 Expression by *PtROS1*-RNAi Affects DNA Methylation in Constitutive Ribosomal DNA and Heterochromatin

Previously, it has been shown that cytosine methylation in poplars correlates with pleiotropic phenotypic changes (Zhu et al. 2013). Therefore, we decided to analyze the cytosine methylation in transformant poplars with *PtROS1*-RNAi construct. The status of highly repetitive 163-bp *5.8S* rDNA was analyzed to study how the silencing of *ROS1* gene cause to methylate constitutive heterochromatin. The methylation can be developed on both cytosines in the CpHpG and CpG and we detected the heavily methylated cytosine using the

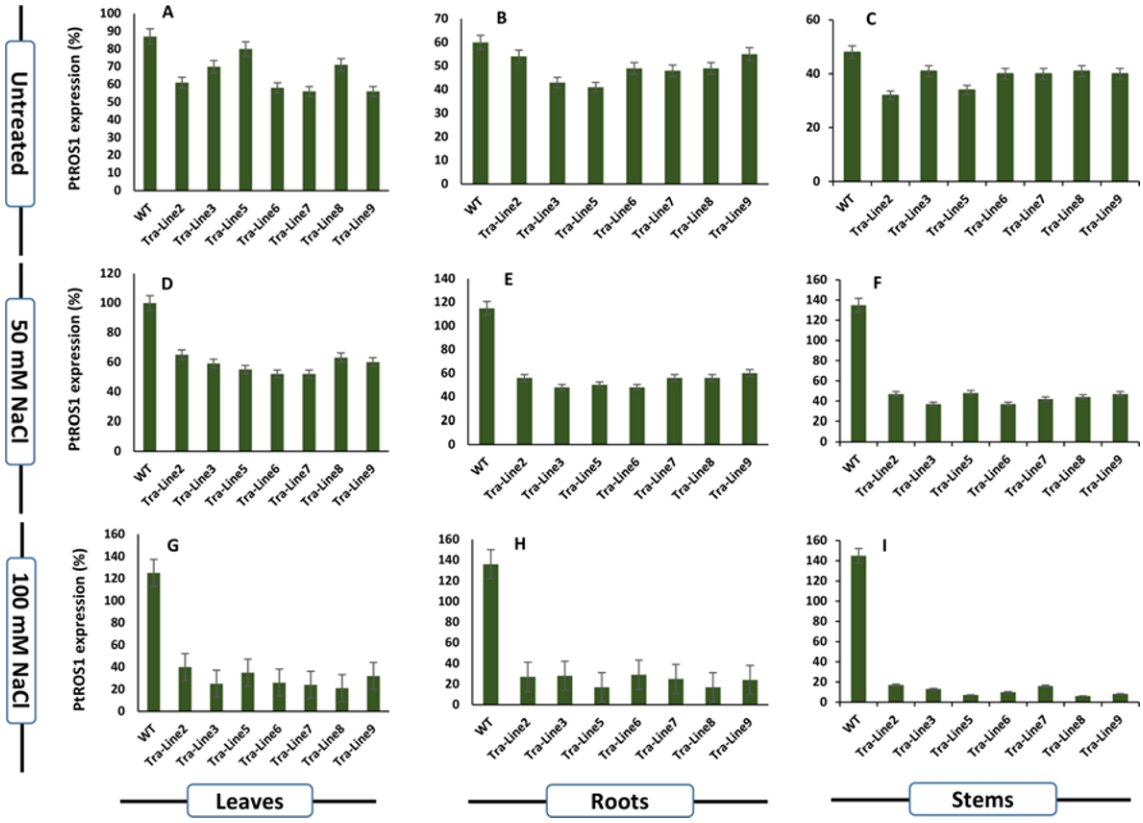

Fig. 5. Endogenous *PtROS1* expression in *PtROS1*-RNAi transgenic lines vs. non-transgenic controls (WT) as determined by qPCR. All the represented transformant lines showed significant reduction in the *PtROS1* expression especially under different salt treatments; (A-C) represent the expression of *PtROS1* in leaves, roots and stems under 0 mM NaCl treatment, respectively. (D-F) represent the expression of *PtROS1*, under 50 mM NaCl treatment. (G-I) represent the expression of *PtROS1*, under 100 mM NaCl treatment. Three independent repeats were carried out for each experiment included five biological replicates; bars represent standard errors.

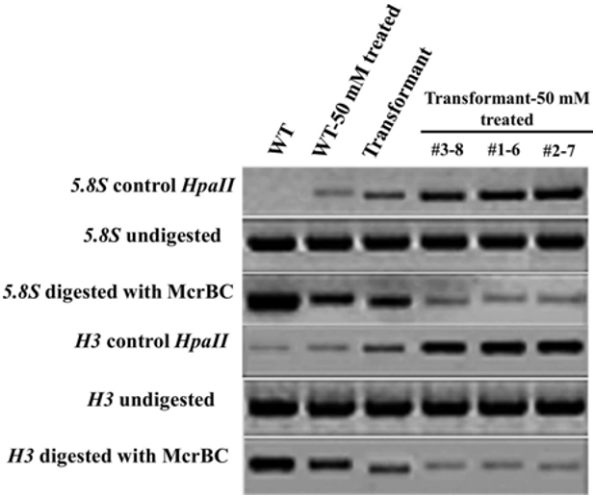

Fig. 6. DNA methylation status. The *5.8S* and *H3* histone genes, which lack *Hpa*II sites, served as a PCR control. Identical quantities of undigested DNA were used as controls for evaluating methylation of the *5.8S* and *H3* genes digested by McrBC. Numbers above lanes refer to the individual plants.

McrBC and methylation sensitive isoschizomers *Msp*I and *Hpa*II enzymes.

*Msp*I can cleave unmethylated symmetric CpG (e.g., CCGG) sequences, and also methylated C_mCGG in half (only one strand DNA) or completely (double strand DNA), but not methylated $_mCCGG$ and $_mC_mCGG$ in half or completely sequences. Whereas, *Hpa*II can only cleave unmethylated symmetric CpG and half methylated $_mCCGG$ sequences (Zhu et al. 2013).

As shown in Fig. 6, digested genomic DNA by *Hpa*II from WT poplars, specifically in *5.8S* and *H3* loci, revealed absent or low intense bands comparing with all transformants introduced by 50 mM NaCl (#3-8, #1-6, and #2-7), regarding to undigested loci. Inversely, digested genomic DNA by McrBC revealed low intense bands in transformants in comparing with WT poplars.

Southern blot analysis of genomic DNA digested with *Hpa*II exhibited enhanced DNA methylation in CpG and CpHpG sites in transformants introduced by 50 mM NaCl affected by repression of *PtROS1* compared to WT poplars regarding to the control (*ycf4*). These analyses also proved increasing of NaCl enhanced DNA methylation especially in transformants in against with WT poplars (Fig. 7).

Methylation of histone *H3* gene was analyzed by RE-

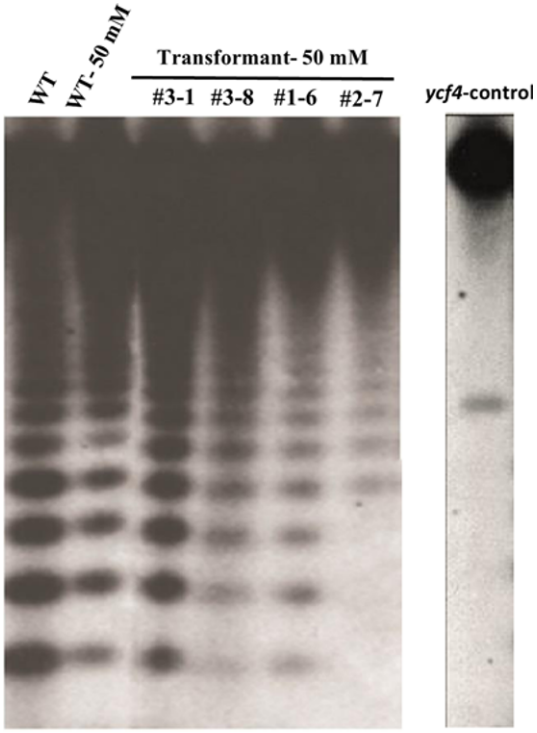

Fig. 7. DNA methylation of 163-bp repeat fragments as determined by Southern blot analysis. Genomic DNA was digested with *Hpa*II (CCGG). Methylation of CpG and CpHpG sites, which are not cleaved by *Hpa*II, was increased dramatically in transformants. DNA methylation was increased non-significantly in WT poplars treated with NaCl, compared with untreated WT poplars. *Ycf4* gene was probed as control. Numbers above lanes refer to the individual plants used in Fig. 5.

qPCR using *ScrF*I (CCNGG) and *Msp*I/*Hpa*II (CCGG). Genomic DNA was digested and amplified using primers flanking the digestion sites (Fig. 8A). Analysis of cytosine methylation with *Msp*I digestion showed a non-significant increase in three transformants (plants 1-8, 1-5, and 1-9) compared to the WT (Fig. 8B). Analysis of cytosine methylation with *Hpa*II digestion indicated hypermethylation of CpG and CpHpG sites in histone *H3* locus. Methylation was increased significantly in transformants (plants 1-8 and 1-5) compared to the WT (Fig. 8C). Analysis of cytosine methylation with *ScrF*I digestion showed asymmetric methylation (CCNGG) on histone *H3* gene. Cytosine methylation was increased significantly in two transformants (plants 1-5 and 1-9) compared to the WT (Fig. 8D).

DNA Methylation at *5.8S* rDNA and Histone *H3* Loci

We assayed the effect of the *PtROS1*-RNAi construct on methylation of the *5.8S* rDNA and histone *H3* genes outside of centromeres in *Populus* Nanlin895 genomic DNA using genomic bisulfite sequencing. Treatment with 0, 50, and 100 mM NaCl was performed to investigate the effect of environmental stresses on cytosine methylation in WT and *PtROS1*-RNAi transformant poplars regarding to the *ycf4* gene as control. Our results showed that leaves of WT and transformant poplars showed more (%) methylated symmetric CpG sites than roots and stems via 0, 50 and 100 mM NaCl treatments (Fig. 9). Leaves of transformants revealed the

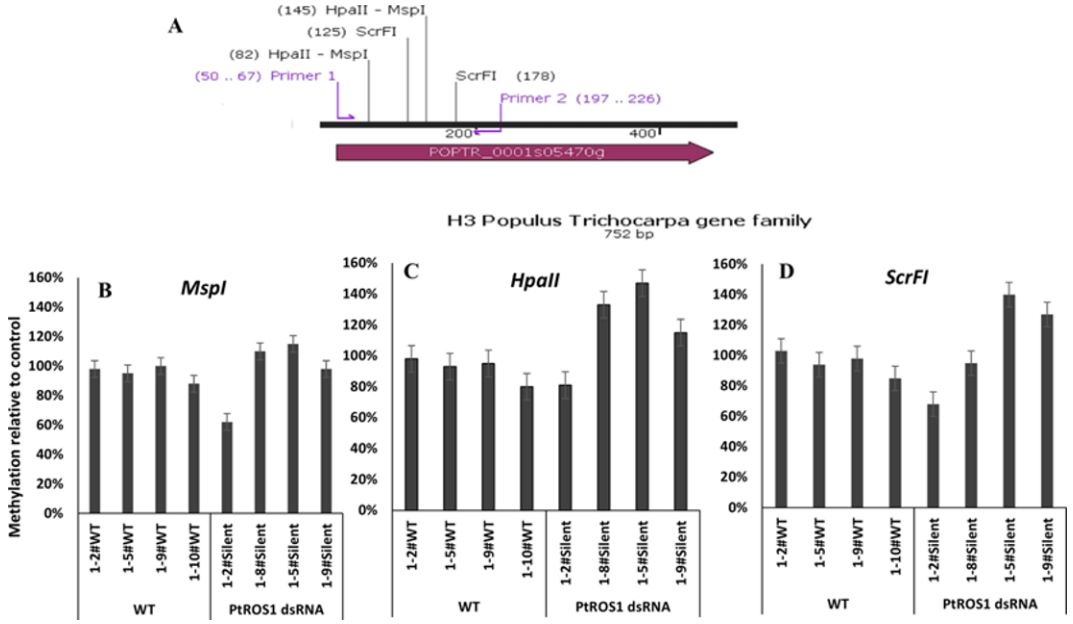

Fig. 8. Methylation of histone *H3* DNA. Genomic DNA was digested with *Msp*I, *Hpa*II, or *ScrF*I and amplified using primers flanking the digestion sites. (A) Diagram of the analyzed sequence, with primers and *ScrF*I and *Msp*I/*Hpa*II restriction sites marked. (B) Results of *Msp*I digestion showing methylation in histone *H3* DNA; the primers flank the two digestion sites. (C) Results of *Hpa*II digestion showing CpG and CpHpG methylation in histone *H3* DNA. (D) Results of *ScrF*I digestion showing asymmetric methylation (CCNGG) in histone *H3*; Data are average of three independent amplifications; error bars represent SD. Numbers refer to the individual plants.

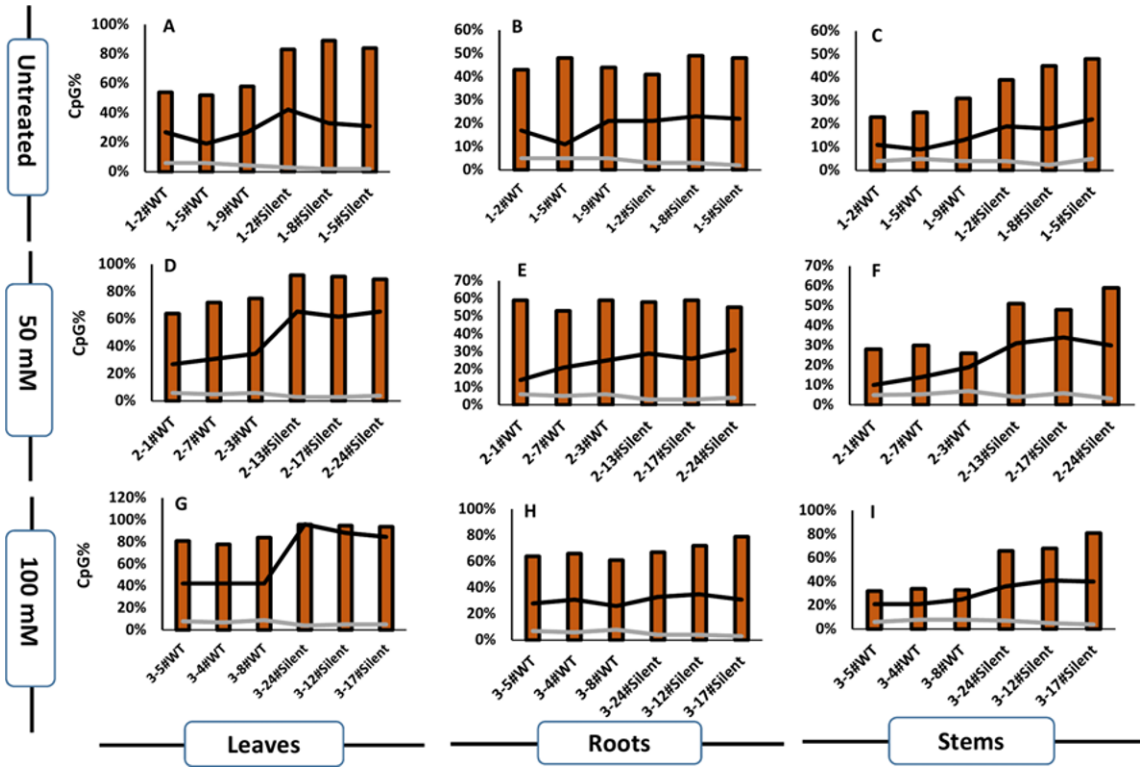

Fig. 9. Genomic bisulfite sequencing of both *5.8S* rDNA and histone *H3* loci following treatment with the indicated NaCl concentrations. (A, D, G) Leaves have shown more methylated CpG sites in transformants than WT poplars in both *5.8S* rDNA and histone *H3* genes under all NaCl treatments. (B, E, H) Roots have shown no more increase methylated CpG sites in transformants than WT poplars in both *5.8S* rDNA and histone *H3* genes under all NaCl treatments. (C, F, I) Stems have shown more methylated CpG sites than WT poplars in both *5.8S* rDNA and histone *H3* genes under all NaCl treatments. Columns represent the percent of CpG sites in *5.8S* rDNA loci; Lines represent the percent of CpG sites in histone *H3* loci. Numbers refer to the individual plants used in Fig. 7 added by random individual transformants from line 2 and 3 to introduce NaCl treatment.

average of methylated CpG sites ~85% and ~35% in *5.8S* rDNA and histone *H3* compared to ~55% and 24% respectively, in WT poplars (Fig. 9A). Roots of transformants and WT poplars revealed the same average of methylated CpG sites ~45% in *5.8S* rDNA loci, while histone *H3* included only ~16% methylated CpG sites in WT poplars and ~22% in transformants (Fig. 9B). It has been shown that stems of transformants contain more methylated CpG sites ~44% and ~20% in *5.8S* rDNA and histone *H3* respectively, comparing by 26% and 11% in WT poplars (Fig. 8C). Under 50 mM NaCl treatment, leaves of transformants exhibited more methylation on CpG sites ~91% and 64% in *5.8S* rDNA and histone *H3* respectively, than ~70% and 31% in WT poplars (Fig. 9D). Increasing of NaCl treatment to 50 mM NaCl caused to enhance methylation in roots and stems similar to leaves. Roots of transformant and WT poplars exhibited the same average of methylated CpG sites ~57% in *5.8S* rDNA, while histone *H3* in transformants revealed the average of methylated CpG sites by ~30% comparing by ~20% in WT poplars (Fig. 9E). Also, stems of transformants exhibited the averages of methylated CpG sites by ~53% and ~32% in *5.8S* rDNA and histone *H3* comparing with ~28% and ~14% in WT poplars (Fig. 9F). Our results proved that the 100 mM NaCl treatment cause to hypermethylate *5.8S* rDNA and histone *H3* in the loss-of-function of ROS1 in *PtROS1*-RNAi transformant poplars. Leaves of transformants exhibited the most averages of methylated CpG sites in our analyses by ~95% and ~90% in *5.8S* rDNA and histone *H3*, comparing by ~81% and ~42% in WT poplars (Fig. 9G). Roots of transformants revealed the average of methylation on CpG sites by ~73% and ~33% in *5.8S* and histone *H3*, compared to ~64% and ~28% in WT poplars (Fig. 9H). Also, results showed more the averages of methylated CpG sites in roots of transformants by ~72% and ~39% throughout *5.8S* rDNA and histone *H3*, compared to ~33% and ~22% in WT poplars (Fig. 9I). The homogenous distributions of methylated CpG sites were shown throughout both *5.8S* rDNA genes in WT and transformant poplars (Fig. S8A, B) and histone *H3* (Fig. S9A, B) regarding to the *ycf4* gene as control (Fig. S10A, B).

Furthermore, genomic bisulfite sequencing was carried out to analyze asymmetric CpHpG and CpHpH contexts for both *5.8S* rDNA and histone *H3* in WT and transformant poplars regarding to the *ycf4* gene as control. Untreated WT poplars exhibited the average of methylated CpHpG sites by

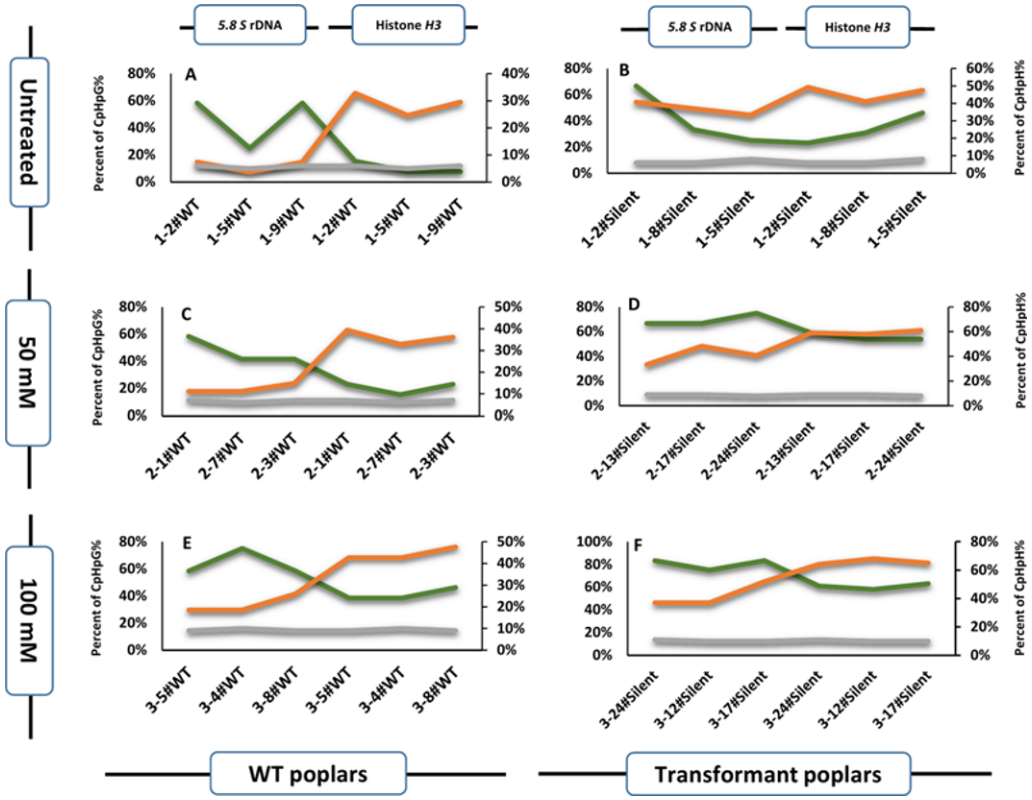

Fig. 10. Genomic bisulfite sequencing of both *5.8S* rDNA and histone *H3* loci following treatment with the indicated NaCl concentrations. (A, B) Untreated transformants (1-2, 1-5 and 1-8) revealed more (%) methylated CpHpG and CpHpH contexts than untreated WT poplars (1-2, 1-5 and 1-9) in both *5.8S* rDNA and histone *H3* loci. (C, D) 50 mM NaCl treated WT poplars (2-1, 2-7 and 2-3) showed more methylated CpHpG and CpHpH contexts than untreated WT poplars. Furthermore, 50 mM NaCl treated transformant trees (2-13, 2-17 and 2-24) showed more methylated CpHpG and CpHpH contexts than the same treated WT poplars in both *5.8S* and *H3* genes. (E, F) Under 100 mM NaCl treatments, both WT (3-4, 3-5 and 3-8) and transformant (3-24, 3-12 and 3-17) poplars revealed more methylated CpHpG and CpHpH contexts than 50 mM NaCl treated trees in both *5.8S* and *H3* genes. Also, transformants showed more methylated CpHpG and CpHpH contexts than WT poplars in *5.8S* and *H3* genes. Dark lines represent CpHpG contexts; Light lines represent CpHpH contexts. Numbers refer to the individual plants used in Fig. 8.

~47% and 10% and methylated CpHpH sites by ~6% and ~29% throughout *5.8S* rDNA and histone *H3* loci (Fig. 10A), while untreated transformants revealed the average of methylated CpHpG sites by ~42% and ~33% and methylated CpHpH sites by ~37% and ~46% throughout *5.8S* rDNA and histone *H3* loci (Fig. 10B). 50 mM NaCl treated WT poplars exhibited the average of methylated CpHpG sites by ~47% and ~20% and methylated CpHpH sites by ~12% and ~36% throughout *5.8S* rDNA and histone *H3* (Fig. 10C), while 50 mM NaCl treated transformants showed more asymmetric methylated CpHpG by ~70% and ~56% and methylated CpHpH sites by ~41% and ~59% throughout *5.8S* and histone *H3* loci (Fig. 10D).

100 mM NaCl treatments caused to hypermethylate transformants in *5.8S* rDNA. 100 mM NaCl treated WT poplars showed the averages of methylated CpHpG sites by ~64% and ~41% and methylated CpHpH sites by ~21% and ~45% throughout *5.8S* rDNA and histone *H3* genes (Fig. 10E), while 100 mM NaCl treated transformant poplars exhibited hypermethylated CpHpG sites by ~80% and ~61% and methylated CpHpH sites by ~42% and ~66% throughout *5.8S* rDNA and histone *H3* loci (Fig. 10F).

Pleiotropic Abnormalities Correlated with Reduced ROS1 Expression

The transformants with greater reductions in *PtROS1* homolog expression exhibited marked phenotypic abnormalities compared with the transformants with a smaller reduction in *PtROS1* homolog expression, and with the WT (Fig. S11). Treatment of the transgenic poplars with three levels of NaCl treatment (0, 50 and 100 mM) resulted in a reduction by ~60% in shooting (%) and a reduction by ~50% in rooting (%) whereas, WT poplars respectively presented a reduction by ~50% and ~50% (Fig. 11A, B). However, the transformants exhibited increase by ~37% in the late shooting (%) and by ~27% in the late rooting (%) via NaCl treatment (0, 50 and 100 mM) compared with WT poplars that exhibited increase

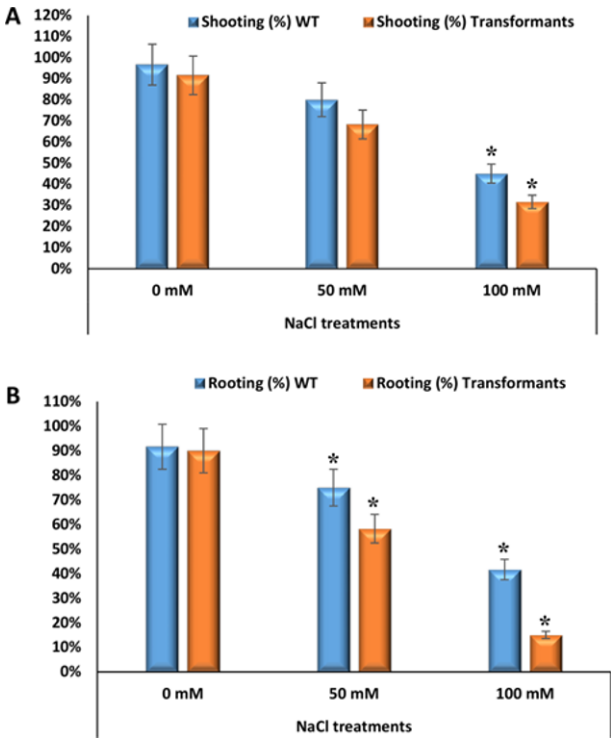

Fig. 11. Phenotypic analyses of *PtROS1*-RNAi poplars versus WT. (A) The shooting of transformants has been significantly decreased comparing with WT poplars in 100 mM NaCl treatment while there was no significant difference between WT and transformants in 0 and 50 mM NaCl treatments. (B) The rooting of transformants has been significantly decreased respectively via 50 and 100 mM NaCl treatments compared to WT poplars. Asterisks indicate significant differences; three independent repeats were carried out for each experiment included five biological replicates; bars represent standard errors.

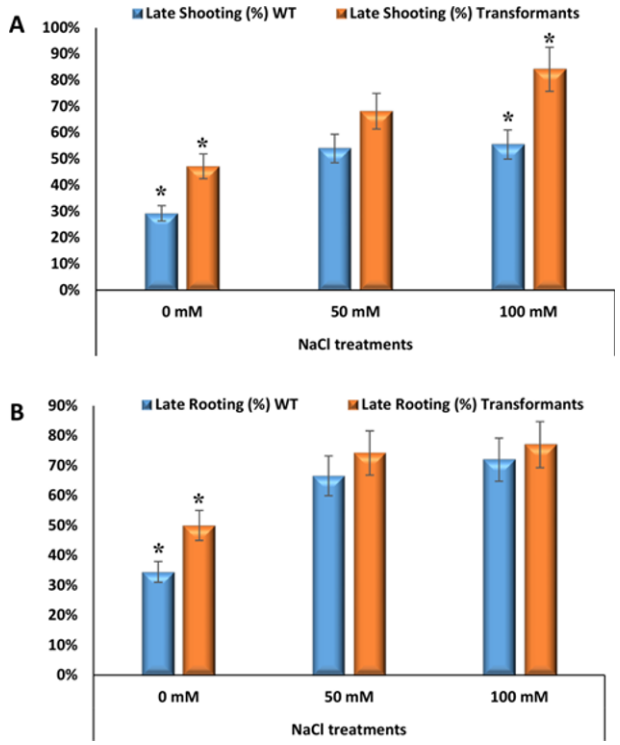

Fig. 12. Phenotypic analyses of *PtROS1*-RNAi poplars versus WT. (A) The late shooting has been significantly increased in transformants vs. WT poplars in common conditions (0 mM) and 100 mM NaCl treatments respectively. (B) The results of late rooting presented significant difference between WT and transformant poplars only via common conditions (0 mM NaCl treatments). Asterisks indicate significant differences; three independent repeats were carried out for each experiment included five biological replicates; bars represent standard errors.

by ~27% in the late shooting (%) and by ~38% in the late rooting (%) (Fig. 12A, B). Also, the reduction of size in transgenic poplars was increased by ~75% via three levels of NaCl treatment (0, 50 and 100 mM) whereas, WT poplars revealed a reduction of size by ~56% (Fig. 13). Also, we observed significant increase in the number of leaves in transgenic poplars compared to WT types and finally, the wavy leaves (%) was increased by ~28% in transgenic poplars against to ~45% in WT types via three levels of NaCl treatments (0, 50 and 100 mM) (Fig. 14). It has been shown that phenotypic changes are correlated with the downregulation of *ROS1* gene and the interference with *ROS1* gene expression lead to pleiotropic changes of phenotype in poplars.

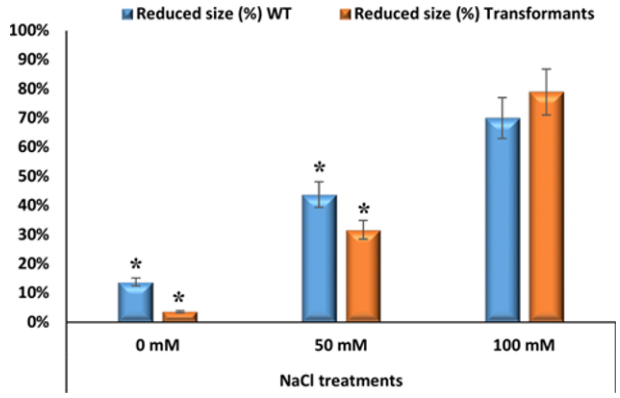

Fig. 13. Phenotypic analyses of *PtROS1*-RNAi poplars versus WT. The results of reduced size presented statistical decrease respectively in 0 and 50 mM NaCl treatments in transformants against to WT poplars. Reversely, it was observed no statistical increased reduced size in transformants comparing with WT poplars in 100 mM NaCl treatment. Asterisks indicate significant differences; three independent repeats were carried out for each experiment included five biological replicates; bars represent standard errors.

Discussion

The ROS1 and DME are potential DNA glycosylases. ROS1 and DME recruit the base excision repair system to remove one free 5-methyle cytosine and make a gap through sequence of DNA, leading to replace an unmethylated cytosine (Kapoor et al. 2005). In addition, recent researches confirmed that in

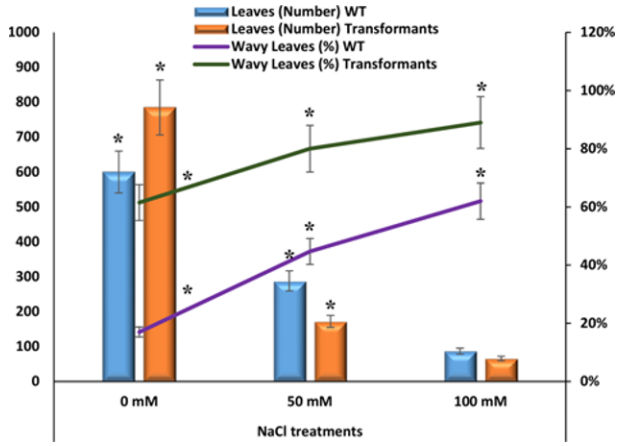

Fig. 14. Phenotypic analyses of PtROS1-RNAi poplars versus WT. The number of leaves has been shown statistically increased in transformants comparing with WT poplars in common conditions (0 mM NaCl treatment), while it has been dramatically decreased in transformants comparing with WT poplars in 50 mM NaCl treatment. The results of wavy leaves presented significant differences in transgenic plants respectively in 0, 50 and 100 mM treatments versus WT poplars. Asterisks indicate significant differences; three independent repeats were carried out for each experiment included five biological replicates; bars represent standard errors.

Arabidopsis, *ros1* exhibits a base excision repair mechanism by DNA glycosylase activity resulting in counteracting RdDM (Mehrotra and Goyal 2014; Zhang et al. 2015). Abiotic stresses such as osmotic inducers make heterochromatic loci via hypermethylation DNA (Li and Tollefsbol 2011). Furthermore, other abiotic stresses such as drought and salt stresses induce metabolic changes associated with hypermethylation on CpHpG sites particularly in satellite DNA (Mehrotra and Goyal 2014; Zhang et al. 2015).

We designed a *PtROS1*-RNAi construct to suppress its homolog expression in Nanlin895 poplar, and investigated the effect on cytosine methylation under normal conditions and in response to salinity stress. Furthermore, we evaluated the effect of suppression of ROS1 on hypermethylation in poplar and phenotypic changes.

Quantitative PCR has been carried out to compare the expression of *PtROS1* in WT and transformant poplars between leaves, roots and stems. Our results proved that Leaves display more expression of *ROS1* than roots and stems under 0, 50 and 100 mM NaCl treatments. Moreover, all the *PtROS1*-RNAi transgenic poplars exhibited the reduction in expression of *ROS1* compared to control (WT poplars). The maximum reduction of expression has been represented in stems. In addition, increase of NaCl treatments caused to demote the expression of *ROS1* in transgenic plants, while WT poplars showed the promoted expression of *ROS1*. Our results proved that environmental stresses such as salinity, induces the expression of *ROS1* to prevent of methylation DNA. According to (Movahedi et al. 2015a), a balance is maintained between DNA methylation (mediated by the RdDM pathway, including RDM1, CMT3, DRM1), and DNA demethylation (mediated by ROS1 and DME, which are stimulated by environmental stresses, such as NaCl).

Our analyses on methylated CpG sites proved that NaCl treatment induces methylation on CpG sites in poplars. It has been shown that hypermethylation on CpG sites was occurred in leaves under 100 mM NaCl treatment. Results proved that leaves exhibit more methylation than roots and stems under common condition (0 mM NaCl treatment) or induced by stresses (50 and 100 mM NaCl treatments). Furthermore, it has been shown that *5.8S* rDNA genes were methylated on CpG sites more than histone *H3* in WT and transgenic poplars. *PtROS1*-RNAi transgenic plants displayed more methylated CpG sites than WT poplars in *5.8S* rDNA and histone *H3*. The minimum of methylation of DNA was occurred in stems of WT poplars with less than ~11% methylated CpG sites throughout histone *H3* in common conditions. Whereas, the maximum of methylation of DNA (Hypermethylation) was occurred in *PtROS1*-RNAi transgenic plants with more than ~95% methylated CpG sites throughout *5.8S* rDNA and induced by 100 mM NaCl treatment. Furthermore, roots exhibited middle methylated CpG sites in WT and transformants through *5.8s* and *H3* genes, while stems represented the lowest methylated CpG sites in WT and transformant poplars through *5.8S* and *H3* genes.

The monitoring of asymmetric CpHpG and CpHpH sites exhibited that methylation on CpHpG sites in *5.8S* rDNA was more than histone *H3* in WT and transformant poplars. Our results showed that methylated CpHpG contexts were increased via NaCl treatments. On the other hands, our results revealed that methylation on CpHpH sites through histone *H3* loci was more than *5.8S* rDNA loci in WT and transformant poplars. The maximum of methylation of DNA on CpHpG contexts in transformant poplars was happened through *5.8S* rDNA by more than ~80% in 100 mM NaCl treatment, while the minimum of methylation of DNA on CpHpG sites in WT poplars was occurred through histone *H3* by less than ~10% in common condition. Therefore, our results proved that *PtROS1*-RNAi poplars in loss-of-function of ROS1 revealed more methylated CpHpG sites than WT poplars through *5.8S* rDNA loci and these methylation was increased via NaCl treatments. Although, *5.8S* rDNA exhibited more methylated CpHpG contexts than histone *H3* in WT and transformant plants, but the maximum methylation of DNA on CpHpH sites was happened in transformants by more than ~66% through histone *H3* in 100 mM NaCl treatment. Furthermore, the minimum methylation of DNA on CpHpH sites was recorded in WT poplars by less than ~6% through *5.8S* rDNA in common condition.

In WT poplars, the maximum methylated CpHpH sites was recorded in histone *H3* by more than ~45% in 100 mM

NaCl treatment, whereas in the same condition the maximum methylated CpHpG sites was happened in *5.8S* rDNA by more than ~64%. Furthermore, in transformant poplars, the maximum methylated CpHpH sites was observed in histone *H3* by more than ~66% in 100 mM NaCl treatment, whereas the maximum methylated CpHpG sites was observed in *5.8S* rDNA by more than ~80% in the same condition. In total, our results proved that asymmetric methylated sites revealed different levels of cytosine methylation, which are dependent on their loci on the genome.

Pleiotropic analyses in WT poplars revealed more shooting (%) and rooting (%) compared to transgenic plants via NaCl treatments (0, 50 and 100 mM). Our observation of shooting (%) revealed a significant differences between WT and transgenic poplars in 100 mM NaCl treatment. Also, our observation of rooting (%) revealed significant differences between WT and transgenic poplars in 50 and 100 mM NaCl treatments. These results proved that ROS1 protein has a key role in shooting and rooting in plants and this role is more important when plant is exposed by environmental stresses. In addition, the results of late shooting (%) and late rooting (%) revealed an increased percentage in transgenic poplars versus WT plants and confirmed the important role of ROS1 protein in shooting and rooting in plants. Furthermore, analyses on leaves revealed that in common condition (0 mM NaCl treatment) the repression of ROS1 protein resulted in increasing the number of leaves significantly, but it was dramatically decreased in 50 mM NaCl treatment. These results showed that the balance between methylation and demethylation of DNA during cell division is necessary for generating of plant leaves. The loss-of- function of *ROS1* gene in 50 mM NaCl treatment cause to hypermethylate of DNA resulted in decreasing of generation of plant leaves. These abnormalities also has been observed in wavy leaves (%). The results of wavy leaves (%) revealed an increased percentage in transformant poplars comparing with WT via NaCl treatments (0, 50 and 100 mM NaCl).

Finally, our analyses of cytosine methylation in WT and *PtROS1*-RNAi transformant poplars showed that methylation of *5.8S* rDNA and histone *H3* genes was downregulated by *ROS1* gene, and suppression of *ROS1* gene resulted in hypermethylation of DNA, particularly of repetitive sequences and cause to reveal abnormalities phenotypic changes in plants.

Materials and Methods

Sequence Analysis and Plasmid Construction

We identified a putative ROS1 protein from the *Populus trichocarpa* genome (POPTR_0006s11720g) in the Uniprot database (http://www.uniprot.org/) and performed a Blastp search of the database of annotated genes (http://blast.ncbi. nlm.nih.gov/Blast/) for similarity to the ROS1 domain. The *P. trichocarpa* ortholog of the ROS1 protein in *Populus euphratica* (>96% identify and 100% query cover) was assumed to be the PtROS1 protein and we performed an alignment of ROS1 proteins from various species to identify a consensus sequence. Total RNA was extracted from *P. trichocarpa* using TRIzol reagent (Tiangen Biotech, Beijing, China) and DNaseI (NEB, USA), according to the manufacturer's instructions, and the quality of RNA was assessed using a BioDrop spectrophotometer (UK). The PrimeScript One-Step RT-PCR ver. 2 Kit (Takara Biotechnology, Dalian, China) and oligo-dT primers were used to synthesize cDNA from 3 μg of extracted RNA according to the manufacturer's instructions. The putative *PtROS1* sequence was amplified from *P. trichocarpa* using degenerate primers (CLC Genomics Workbench 3 software, Taipei, Taiwan) and cloned into the pEASY-T3 cloning vector (pEASY-T3 cloning kit) using the TA cloning technique. The sequence was submitted to the National Center for Biotechnology Information (NCBI) under accession number KU587630. The Vector NTI ver. 11 software (http://www.invitrogen.com/) was used to design a RNAi construct to suppress *PtROS1* transcripts in the target hybrid clone *P. deltoides* × *P. euramericana* 'Nanlin895' poplar, which is widely used for poplar transformation (Zhu et al. 2013; Movahedi et al. 2015b; Movahedi et al. 2015c). In this research, the established RNA interference (RNAi) has been used to knock-down the transcribed *PtROS1* (Camargo et al. 2016; Meng et al. 2017). For using a dsRNA approach to silence PtROS1 expression in Nanlin895, we ligated 129-bp gene-specific DNA fragments isolated from the cDNA of *P. trichocarpa* in both antisense and sense orientations into the pGWB9 expression vector (accession number AB289772). The transcribed RNA from this construct was able to form a dsRNA with a single-stranded loop terminal resulting in silencing of ROS1. A total of 270 transformants was generated in nine independent lines (each line included 30 individuals). The 843-bp *PtROS1*-RNAi construct included a 210-bp pyruvate dehydrogenase kinase (pdk) intron flanked by two 129-bp open reading frame (ORF) fragments from cDNA extracted from *P. trichocarpa* corresponding to positions 2386–2514 bp in the sense and anti-sense orientations and a 253-bp *NOS* terminator fragment. This 129-bp fragment was investigated by Geneious version 10.2 created by Biomatters to analyze the off-targets. The *PtROS1*-RNAi caset was sequenced and prepared by GeneScript ® Company and ligated in pUC57 vector. The *PtROS1*-RNAi construct was amplified from pUC57 vector using the forward primer 5'-atgattacgccaagcttaggcct-3' and the reverse primer 5'-gcgatcgcggggtaagg-3' (SnapGene 1.1.3, Chicago, USA) flanked by *Hind*III and *Asi*SI restriction sites, then cloned into the pGWB9 expression vector at positions 4950–5795 bp in the sense orientation. Expression of the *PtROS1*-RNAi silencing construct was driven by CaMV *35S* promoter. The orientation of the cloned DNA fragment in the final expression vector was confirmed by restriction analysis and sequencing.

To investigate *PtROS1* gene expression based on biological processes and molecular function, we carried out Gene Ontology (GO) analysis (An approved representation of a biological processes, functions and cellular components, within a given domain) of plant ROS1 orthologs included in a phylogenetic tree.

Plant Transformation

Transformation of *P. deltoides* × *P. euramericana* 'Nanlin895' poplar was performed using *Agrobacterium tumefaciens* strain EHA105 as described by Movahedi et al. (2015b). Transgenic plants were selected with 100 mg mL^{-1} kanamycin. Poplar plants were cultured and grown on Murashige and Skoog (MS) medium supplemented by light for 16 h at 23°C. To identify transgenic poplar plants, 1 μg of genomic DNA (BioDrop spectrophotometer, UK) was extracted using the cetyltrimethylammonium bromide (CTAB). PCR was performed with the forward primer 5'-atgattgaacaagatggattgcacgc-3' of neomycin phosphotransferase II (*NPT* II) gene and the reverse primer 5'-

cctagagatccgtcaacatggtgg-3' of CaMV *35S* promoter. The amplified fragments (3764 bp) were then resolved in a 1.5% agarose gel. The purified bands then have been sent to GeneScript ® Company to sequence and verify. Kanamycin-resistant plants were regarded as transgenic.

RT-PCR Gene Expression Analysis, SDS-PAGE and Western Blotting

Total RNA was extracted from young leaves of putative *PtROS1*-RNAi transformants and WT poplars using a plant RNA kit (Omega Biotech No: R6827-01, China) and digested with DNase I (Takara Biotechnology, China). cDNA was synthesized using the PrimeScript One Step RT-PCR Ver. 2 Kit (Takara Biotechnology, Dalian, China) and stored in TE buffer. Specific primers of *β-actin* (Accession number: XM-006370951.1), forward 5′-gaccttcaatgtgcctgcaa-3′ and reverse 5′-accatcaccagaatccagca-3′, were used to normalize the cDNA concentration in PCR reactions. Specific primers of full length cDNA of *PtROS1* gene were used (Forward 5'-atgccttcactactatttcgaaagaaaaagagg-3' and reverse 5'-ctaccga- ccactaatatcacacttttttgtctg-3') to evaluate expression in WT and *PtROS1*-RNAi transgenic poplar plants. A PCR linearity control was performed for each reaction using control cDNA. In addition, the intensity of bands were measured using the ImageJ ver. 1.5b software.

Furthermore, SDS-PAGE was performed according to Zhang et al. (2015). Total protein was extracted from matured leaves using extraction buffer (Tric-Hcl 1.5 M pH8.8 100 mM, EDTA 10 mM, Sucrose 0.9 M, 2-mercaptoethanol 0.4%), saturated phenol pH8.8, protein precipitation buffer (Methanol absolute, Ammonium acetate 100 mM), washing buffer (Acetone 90%, DDT 10 mM), and lysis buffer (Tris-base 35 mM, Urea 7M, Thiourea 2M, CHAPS 4%, DDT 0.002%). The Bradford assay was then carried out to quantify proteins and SDS-PAGE was performed to dissolve protein samples and detect the expression of PtROS1 in WT and transformant plants. Finally, comassi blue R-250 was used to stain the gel and observe. In addition, 10 μg of extracted proteins were separated by 10% SDS-PAGE to transfer onto PVDF membrane. The anti-ROS1 (Anti-body ab181113) were then used to detect ROS1 protein among WT and transformant poplars.

Quantitative Real-time PCR

According to Gao et al. (2010) ROS1 demethylates *RDM1* gene involved in RdDM pathway leading to balance. To assay demethylase activities of PtROS1, We carried out restriction enzyme quantitative real-time PCR (RE-qPCR) using digested genomic DNA by *Hpa*II (sensitive methylation) to prime *PtRDM1* gene with the accession number KT633998 (Forward 5'-tgaactggagtgtggtgatctctg-3' and reverse 5'-attcaa ccagacaaggaatattttaa-3'). In addition, *ycf4* gene, which is one photosystem I gene isolated from chloroplast with a low stable cytosine methylation via stresses (Omidvar and Fellner 2015), has been probed (Forward 5'-attagctcttatttgtggtgca-3' and reverse 5'-tcaaaatacttcaattggtacacgc-3') to use as control. Furthermore, We performed qPCR analysis to quantify endogenous *PtROS1* expression in 0, 50 and 100 mM NaCl treatments, using extracted cDNA of leaves, roots and stems from transgenic (Seven lines included five plants from each line) and non-transgenic (WT) poplars with three technical replicates per reaction. *b-actin* expression was used as an endogenous control according to (Movahedi et al. 2015c). Gene expression in transgenic and WT plants was compared using $\Delta\Delta C_t$ method. A 100-bp fragment of *β-actin* was amplified as the endogenous control using the forward 5′-gaccttcaatgtgcctgcaa-3′ and reverse 5′-accatcaccagaatccagca-3′ primers, which were designed by SnapGene 1.1.3, Chicago, USA. In addition, the forward 5'-atggtgggaagaagaaa-gggcag-3' and reverse 5'-ctagagagatgatctgagacattctgggtaag-3' primers were designed to amplify the 165-bp ORF of the *PtROS1* coding sequence (CDS). Gene expression was calculated according to Zhu et al. (2013).

DNA Methylation Assays

Genomic DNA was extracted using CTAB method from WT and transformants introduced by 50 mM NaCl to perform RE-PCR using *Hpa*II and McrBC enzymes and also southern blot.

1 μg of genomic DNA was digested for 5 h using the DNA methylation endonuclease McrBC, which cleaves methylcytosine at 5'…pumc(N40–3000)pumc…3' sites (http:// www.neb.com) on one or both strands of methylated DNA. Heat inactivation was carried out at 65°C for 20 min and 10% of digested DNA was used for PCR. The following sequences primers then were designed to prime *5.8S* rDNA gene with accession no. AJ006440 (Forward 5'-cgaattcgtg- gtatgatatgttg-3' and reverse 5'-tcgataccgaaaatccgaa-3') and histone *H3* gene with accession no. XM_002299206 (Forward 5'-gttttttttttttttttcgaga-3' and reverse 5'-taaaataataaatctctttcaat-3'). PCR was performed at 95°C for 5 min, followed by 35 cycles of 94°C for 1 min, 55°C for 1 min, and 72°C for 1 min. PCR fragments were then resolved in 1.5% agarose gels.

Southern blot analyses has been carried out using digested genomic DNA by methylation-sensitive *Hpa*II restriction endonuclease. A 163-bp sequence of the repeat fragment of ribosomal DNA was amplified using primers (Forward: 5'-aaacgactctcggcaacgga-3' and reverse 5'-gcgtgacacccaggcag-3') to probe methylated sites throughout the genome. The *ycf4* gene has been probed as control to normalize southern blot (Forward 5'-attagctcttatttgtggtgca-3' and reverse 5'-tcaaaatacttcaattggtacacgc-3').

In addition, genomic DNA was digested by *Msp*I and *Hpa*II (sensitive isoschizomers) and also *ScrF*I to perform one more RE-qPCR for detecting relative DNA methylation on histone *H3* (Forward: 5'-gtttccccctcttttttctcgag-3' and reverse: 5'-aaggtcttcaaattacacttgtg-3').

On the other hands, the EZ DNA Methylation Kit (Zymo Research, USA) has been used to bisulfite sequencing as described by Mehrotra and Goyal (2014). The DNA was amplified by PCR to evaluate the methylation status of the *5.8S* rDNA and histone *H3* genes. The PCR reaction was run for 14 h at 55°C following an initial pre-denaturation at 95°C for 20 min. Converted genomic DNA was then amplified by PCR to evaluate the methylation status of the *5.8S* rDNA and histone *H3* genes (*5.8S* rDNA gene: Forward 5'-cgaattcgtggtatgatatgttg-3' and reverse 5'-tcgataccgaaaatccgaa-3' and histone *H3* gene: Forward 5'-gttttttttttttttttcgaga-3' and reverse 5'-taaaataataaatctctttcaat-3'). The PCR products were purified using the Wizard DNA Cleanup Kit (Promega, Madison, WI, USA) to prevent sequencing errors. Purified PCR products were then separated 2.5% agarose gel and extracted using the QIAquick Gel Extraction Kit (Qiagen, Hilden, Germany), followed by cloning into the pGEM-T Easy vector system II (Promega) and subsequent sequencing of the inserts. The ligated pGEM-T Easy vector was transformed into competent JM109 cells and cultured on Luria-Bertani (LB) agar. Putative transformed white colonies were selected and grown in LB medium, followed by plasmid extraction and sequence analysis. Finally, the BiQ Analyzer ver. 2.0 software was used to analyze cytosine methylation (http://biq-analyzer.bioinf.mpi-inf.mpg.de) in the *5.8S* rDNA and histone *H3* genes.Pleiotropic properties

Approximately 75 individuals of the *PtROS1*-RNAi transformants have been investigated to detect noticeable defects in contrast with WT plants (Controls). During vegetative growth (2-3 months), the pleiotropic properties included shooting (Number of shoots), rooting (Number of roots), late shooting (Number of shoot late regeneration), late rooting (Number of root late regeneration), reduced-size plants, leaves, and wavy leaves were observed and measured.

Statistical Analysis

SPSS ver. 16 and Microsoft Office Excel ver. 2013 software were used to analyze data by one-way ANOVA and Duncan's test. Differences were considered significant with an error value of 0.05 with no overlap in the mean values.

Acknowledgments

This work was supported by the National Science Foundation of China (No. 31570650), the International Science & Technology Cooperation Program of China (2014DFG32440) and the Priority Academic Program Development of Jiangsu Higher Education Institutions.

Author's Contribution

AM designed, performed and directed the experiments, and drafted the manuscript; AM, MS, JZ, KM, WS, AA and SK analyzed the data, and wrote the manuscript; HR and QZ drafted the manuscript. All authors contributed to and approved the final manuscript.

Supporting Information

Fig. S1. Alignment of ROS1 protein in various species of trees.
Fig. S2. Dot and Charge plot analyses of the similarity of PtROS1 and ROS1.
Fig. S3. Strategy for silencing PtROS1 expression.
Fig. S4. The PtROS1-RNAi construct.
Fig. S5. Comparison of expression of genes including on and off-targets.
Fig. S6. Verification of proper ligated plasmid using digestion methods and colony PCR.
Fig. S7. Gene ontology analysis of orthologous groups for ROS1.
Fig. S8. Distribution of DNA methylation at CpG sites in the 5.8S rDNA gene.
Fig. S9. Distribution of DNA methylation on CpG sites in the histone H3 gene.
Fig. S10. Distribution of DNA methylation at CpG sites in ycf4 gene.
Fig. S11. Effect of reduced ROS1 expression on the pleiotropic phenotypes.

References

Agius F, Kapoor A, Zhu JK (2006) Role of the Arabidopsis DNA glycosylase/lyase ROS1 in active DNA demethylation. Proc Natl Acad Sci USA 103:11796–11801

Camargo RA, Barbosa GO, Possignolo IP, Peres LE, Lam E, Lima JE, Figueira A, Marques-Souza H (2016) RNA interference as a gene silencing tool to control Tuta absoluta in tomato (*Solanum lycopersicum*). PeerJ 4:e2673

Choi Y, Gehring M, Johnson L, Hannon M, Harada JJ, Goldberg RB, Jacobsen SE, Fischer RL (2002) DEMETER, a DNA glycosylase domain protein, is required for endosperm gene imprinting and seed viability in Arabidopsis. Cell 110:33–42

Dinh TT, Gao L, Liu X, Li D, Li S, Zhao Y, O'Leary M, Le B, Schmitz RJ, Manavella PA, Li S, Weigel D, Pontes O, Ecker JR, Chen X (2014) DNA topoisomerase 1alpha promotes transcriptional silencing of transposable elements through DNA methylation and histone lysine 9 dimethylation in Arabidopsis. PLoS Genet 10:e1004446

Feng S, Jacobsen SE, Reik W (2010) Epigenetic reprogramming in plant and animal development. Science 330:622–627

Furner IJ, Matzke M (2011) Methylation and demethylation of the Arabidopsis genome. Curr Opin Plant Biol 14:137–141

Gao Z, Liu HL, Daxinger L, Pontes O, He X, Qian W, Lin H, Xie M, Lorkovic ZJ, Zhang S, Miki D, Zhan X, Pontier D, Lagrange T, Jin H, Matzke AJ, Matzke M, Pikaard CS, Zhu JK (2010) An RNA polymerase II- and AGO4-associated protein acts in RNA-directed DNA methylation. Nature 465:106–109

Gehring M, Reik W, Henikoff S (2009) DNA demethylation by DNA repair. Trends Genet 25:82–90

Gong Z, Morales-Ruiz T, Ariza RR, Roldan-Arjona T, David L, Zhu JK (2002) ROS1, a repressor of transcriptional gene silencing in Arabidopsis, encodes a DNA glycosylase/lyase. Cell 111:803–814

Kapoor A, Agarwal M, Andreucci A, Zheng X, Gong Z, Hasegawa PM, Bressan RA, Zhu JK (2005) Mutations in a conserved replication protein suppress transcriptional gene silencing in a DNA-methylation-independent manner in Arabidopsis. Curr Biol 15:1912–1918

Lauria M, Rossi V (2011) Epigenetic control of gene regulation in plants. Biochim Biophys Acta 1809:369–378

Li Y, Tollefsbol TO (2011) DNA methylation detection: bisulfite genomic sequencing analysis Methods. Mol Biol 791:11–21

Lippman Z, Gendrel AV, Black M, Vaughn MW, Dedhia N, McCombie WR, Lavine K, Mittal V, May B, Kasschau KD, Carrington JC, Doerge RW, Colot V, Martienssen R (2004) Role of transposable elements in heterochromatin and epigenetic control. Nature 430:471–476

Lister R, O'Malley RC, Tonti-Filippini J, Gregory BD, Berry CC, Millar AH, Ecker JR (2008) Highly integrated single-base resolution maps of the epigenome in Arabidopsis. Cell 133:523–536

Mehrotra S, Goyal V (2014) Repetitive sequences in plant nuclear DNA: types, distribution, evolution and function. Genomics Proteomics Bioinformatics 12:164–171

Meng F, Li Y, Zang Z, Li N, Ran R, Cao Y, Li T, Zhou Q, Li W (2017) Expression of the double-stranded RNA of the soybean pod borer *Leguminivora glycinivorella* (Lepidoptera: Tortricidae) ribosomal protein P0 gene enhances the resistance of transgenic soybean plants. Pest Manag Sci 73:2447–2455

Movahedi A, Sun W, Zhang J, Wu X, Mousavi M, Mohammadi K, Yin T, Zhuge Q (2015a) RNA-directed DNA methylation in plants. Plant Cell Rep 34:1857–1862

Movahedi A, Zhang JX, Gao PH, Yang Y, Wang LK, Yin TM, Kadkhodaei S, Ebrahimi M, Qiang ZG (2015b) Expression of the chickpea CarNAC3 gene enhances salinity and drought tolerance in transgenic poplars. Plant Cell Tissue Organ Cult 120:141–154

Movahedi A, Zhang JX, Yin TM, Qiang ZG (2015c) Functional Analysis of Two Orthologous NAC Genes, CarNAC3, and CarNAC6 from Cicer arietinum, Involved in Abiotic Stresses in Poplar Plant. Plant Mol Biol Rep 33:1539–1551

Nakashima K, Ito Y, Yamaguchi-Shinozaki K (2009) Transcriptional regulatory networks in response to abiotic stresses in Arabidopsis and grasses. Plant Physiol 149:88–95

Omidvar V, Fellner M (2015) DNA methylation and transcriptomic changes in response to different lights and stresses in 7B-1 male-sterile tomato. PLoS One 10:e0121864

Penterman J, Zilberman D, Huh JH, Ballinger T, Henikoff S, Fischer RL (2007) DNA demethylation in the Arabidopsis genome. Proc Natl Acad Sci USA 104:6752–6757

Questa JI, Fina JP, Casati P (2013) DDM1 and ROS1 have a role in UV-B induced- and oxidative DNA damage in *A. thaliana*. Front Plant Sci 420

Roudier F, Ahmed I, Berard C, Sarazin A, Mary-Huard T, Cortijo S, Bouyer D, Caillieux E, Duvernois-Berthet E, Al-Shikhley L, Giraut L, Despres B, Drevensek S, Barneche F, Derozier S, Brunaud V, Aubourg S, Schnittger A, Bowler C, Martin-Magniette ML, Robin S, Caboche M, Colot V (2011) Integrative epigenomic mapping defines four main chromatin states in Arabidopsis. EMBO J 30:1928–1938

Tariq M, Paszkowski J (2004) DNA and histone methylation in plants. Trends Genet 20:244-251

Vining KJ, Pomraning KR, Wilhelm LJ, Priest HD, Pellegrini M, Mockler TC, Freitag M, Strauss SH (2012) Dynamic DNA cytosine methylation in the Populus trichocarpa genome: tissue-level variation and relationship to gene expression. BMC Genomics 13:27

Zhang J, Movahedi A, Wang X, Wu X, Yin T, Zhuge Q (2015) Molecular structure, chemical synthesis, and antibacterial activity of ABP-dHC-cecropin A from drury (*Hyphantria cunea*) Peptides 68:197–204

Zhang X, Yazaki J, Sundaresan A, Cokus S, Chan SW, Chen H, Henderson IR, Shinn P, Pellegrini M, Jacobsen SE, Ecker JR (2006) Genome-wide high-resolution mapping and functional analysis of DNA methylation in Arabidopsis. Cell 126:1189–1201

Zhu J, Kapoor A, Sridhar VV, Agius F, Zhu JK (2007) The DNA glycosylase/lyase ROS1 functions in pruning DNA methylation patterns in Arabidopsis. Curr Biol 17:54–59

Zhu R, Shevchenko O, Ma C, Maury S, Freitag M, Strauss SH (2013) Poplars with a PtDDM1-RNAi transgene have reduced DNA methylation and show aberrant post-dormancy morphology. Planta 237:1483–1493